Manufacturing Letters 43 (2025) 33–36

Contents lists available at ScienceDirect

Manufacturing Letters

journal homepage: www.elsevier.com/locate/mfglet

Letters

Simultaneous 4D printing and In-Situ foaming for tailoring shape memory behaviors in polylactic acid foams

Pedram Honari [a], Davood Rahmatabadi [a], Abbas Bayati [a], Erfan Rassi [b], Ismaeil Ghasemi [c], Majid Baniassadi [a], Mahdi Bodaghi [d,*], Mostafa Baghani [a,*]

[a] School of Mechanical Engineering, College of Engineering, University of Tehran, Tehran, Iran
[b] Department of Polymer Engineering and Color Technology, Amirkabir University of Technology, Tehran, Iran
[c] Faculty of Processing, Iran Polymer and Petrochemical Institute, Tehran, Iran
[d] Department of Engineering, School of Science and Technology, Nottingham Trent University, Nottingham NG11 8NS, UK

ARTICLE INFO

Article history:
Received 18 August 2024
Received in revised form 10 November 2024
Accepted 30 November 2024
Available online 6 December 2024

Keywords:
Shape memory foam
4D printing
Polylactic acid
Morphology

ABSTRACT

This study introduces an innovative 4D printing technique combined with in-situ foaming to enhance the shape memory properties of polylactic acid (PLA) foams. By melt mixing PLA with azodicarbonamide (AZO) below its decomposition temperature, followed by direct pellet printing, the research achieves uniform microporous structures and tailored shape memory behaviors. The findings demonstrate that higher AZO content improves shape fixity (~96 %) but reduces shape recovery. Moreover, the programming temperature significantly influences performance, with hot programming enhancing shape fixity and cold programming boosting shape recovery. This novel approach offers potential applications in lightweight, thermally insulative, and shock-absorbing materials with programmable properties.

1. Introduction

Polymer foams are one of the most widely used and common polymeric materials characterized by their porous structure. These materials consist of a polymer matrix that contains bubbles of gas encapsulated within it, which can take the form of either open-cell or closed-cell structures. These foams have a wide range of applications in industries such as automotive, furniture, medical, and packaging [1]. They also excel at thermal insulation, are cost-effective, and have a high strength-to-weight ratio [2]. A specific type of advanced polymer foam is shape memory polymer foam, which exhibits not only the benefits of traditional foam, but also shape memory properties. This means that these foams can respond to external stimulus such as heat, electricity, light, and magnetic field changing their shape and then remember the original shape [3].

3D printing techniques, including material extrusion, provide a more cost-effective and customized approach to manufacturing polymeric materials. However, there are still challenges to manufacturing polymer foams using 3D printing techniques. 3D printing of shape memory materials, also referred to as 4D printing, is an innovative technology that can enable the integration of 3D printing capabilities with the unique properties of shape memory polymer foams. This fusion of technologies offers new possibilities for enhancing the functionality of these materials in various fields.

In this pioneering study, the 4D printing of polymer foams is investigated, focusing on the previously unexplored area of shape memory behavior influenced by foaming agent content and programming temperature. Traditional methods for producing shape memory polymer foams often involve complex and costly processes, lacking the precision and customization that 3D printing offers. Polymer foams are typically produced using molding techniques, such as injection molding or compression molding. These methods can produce large quantities of foam, but they require significant investment in tooling and machinery. To address this gap, a novel method for 3D printing polylactic acid (PLA) foams is developed. Unlike previous studies in this field that used filaments, such as gas-saturated filaments for printing foams [4], current method involves melt mixing PLA with azodicarbonamide (AZO) at a temperature below its decomposition point, followed by direct pellet printing at a higher nozzle temperature that induces in-situ foaming.

* Corresponding authors.
E-mail addresses: mahdi.bodaghi@ntu.ac.uk (M. Bodaghi), baghani@ut.ac.ir (M. Baghani).

https://doi.org/10.1016/j.mfglet.2024.11.005

2. Experimental procedure

2.1. Material

PLA pellets (eSun, China) used as the polymer matrix. AZO (Merck, Germany) with starting decomposition temperature of 190 °C, was used as the foaming agent. The PLA/AZO blend were prepared through a melt mixing method. Three different concentrations of AZO, 1 %, 3 %, and 5 %, were employed to investigate their influence on foam morphology and shape memory behavior. In melt mixing method, initially, PLA pellets were melted within the internal mixer at 163 °C (below decomposition temperature of AZO) and a speed of 50 rpm for a period of two minutes. Subsequently, AZO was added to the mixture. The mixture was left in the machine for five minutes to ensure a uniform distribution of the foam agent throughout the polymer matrix. The resulting material was obtained in a lump form, which was subsequently processed using a press machine. A hot press with a temperature of 165 °C and a cold press with a pressure of 60 kPa were employed to transform the lumps into thin sheets with a thickness of 1 mm. The resulting thin sheets were then transformed into granules to serve as feedstock material for direct 3D printing.

2.2. Direct pellet printer

A screw-based pellet printer was employed to directly 3D prints the PLA/AZO granules. This innovative printing technique eliminates the need for filamentation, streamlining the manufacturing process [5]. The printing process was conducted with a nozzle diameter of 0.4 mm, a bed temperature of 50 °C, a layer height of 0.25 mm, and a nozzle temperature of 213 °C. The higher nozzle temperature than the decomposition temperature of the foaming agent allowed for in-situ decomposition of AZO and subsequent foaming of the printed material. The diagram in Fig. 1 shows the design of a screw-based direct pellet printer and its associated foam printing process.

2.3. Characterizations

SEM was employed to investigate the morphology and porosity structure of 3D printed foams. To examine the samples, a Vegall model SEM instrument was employed.

To characterize the viscoelastic properties and transition temperature, a DMTA test was conducted. The test was conducted at a constant frequency of 1 Hz, at a temperature range of 0 °C to 100 °C, with increments of 5 °C/min and under a single cantilever bending load.

The shape memory cycle consists of two primary stages: programming and recovery. Programming can be performed in three different modes: cold, warm, and hot. Cold programming involves loading the material at ambient temperature and then unloading immediately, while warm and hot programming involve additional steps, including heating and cooling [6]. For all samples, a beam with dimensions of 60 x 10 mm and a thickness of 2 mm was printed. The loading process involved bending the printed shape memory samples by 180° at various programming temperatures (cold, warm, and hot). A laboratory-made machine was used to bend the samples at a strain rate of 10°/sec. The shape fixity ratio (Rf) and shape recovery ratio (Rr) can be calculated using the following formulas:

$$R_f = \frac{\theta_{Fixed}}{\theta_{Loaded}} \times 100$$

$$R_r = \frac{\theta_{Recovered}}{\theta_{Loaded}} \times 100$$

3. Results and discussion

3.1. SEM

Fig. 2 shows SEM images of printed PLA foams with varying foaming agent concentrations. As shown, the cavities between deposited rasters and beads, which are always formed in extrusion-based 3D printing due to their layer-by-layer deposition nature, cannot be seen in these samples. This is due to the complete penetration of grids and layers on top of each other. This desirable penetration shows the quality of adhesion between layers and rasters in printed samples.

As depicted in Fig. 2(a–c), PLA-AZO with 1 % wt AZO shows a uniform distribution of spherical micropores with dimensions ranging from 10 to 30 μm. The SEM images confirm that the addition of AZO foaming agent to PLA has produced a uniform distribution of closed holes. The successful production of these holes relies on achieving a uniform reaction temperature during the printing process. The SEM images in Fig. 2(d–f) show PLA-AZO with 3 %

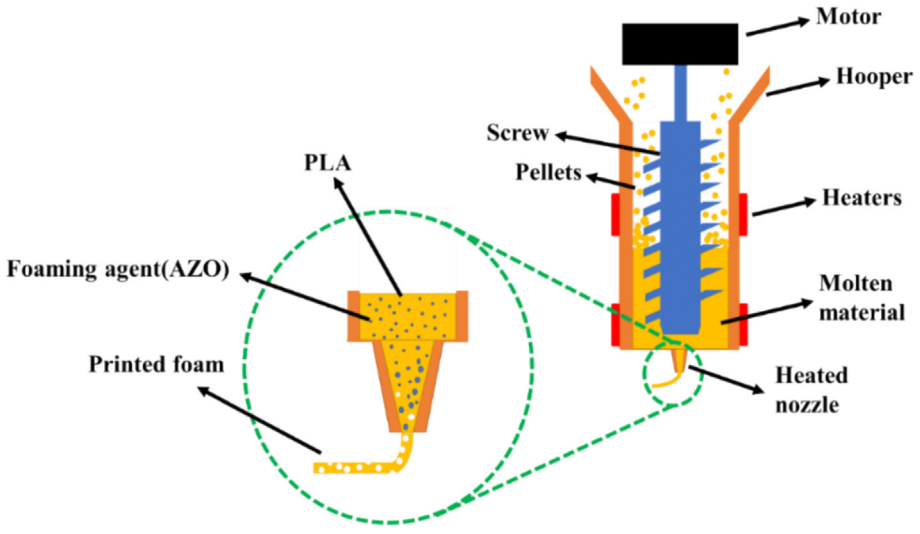

Fig. 1. Direct pellet printer mechanism and foam 3D printing process.

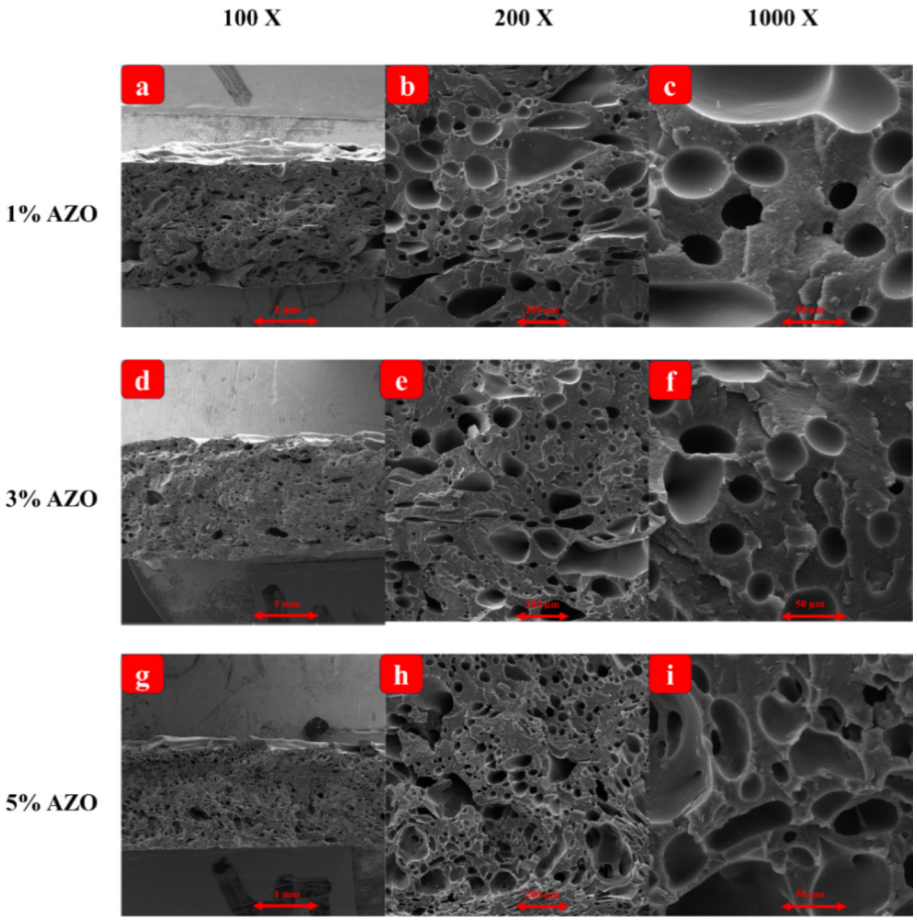

Fig. 2. Morphology of 3D printed PLA with different foam agent concentrations: (a–c) 1 %, (d–f) 3 % and (g–i) 5 % AZO.

wt. The distribution of microholes is still uniform, with spherical shapes and dimensions ranging from 10 to 50 µm. However, some microholes have coalesced in certain areas, resulting in a change in shape from spherical to oval. In PLA-AZO mixture with 5 % wt, despite the increased weight percentage of AZO foaming agent, its performance has not been affected, and it has continued to perform well. This achievement is attributed to the proper distribution of AZO in the PLA matrix, optimal printing quality, and selection of suitable printing parameters. The shape and size of the microholes have also changed, with the holes becoming more elongated. This elongation can be attributed to both extrusion during printing and the coalescence of multiple spherical microholes.

3.2. DMTA

The DMTA of the printed sample is shown in Fig. 3. The glass transition temperature occurs between 60 °C and 80 °C, with a specific glass-rubber transition temperature of 65 °C. This region, known as the "warm region," is marked by a significant decrease in storage modulus, dropping to under 10 MPa. Shape memory programming can occur during this transition state, referred to as "warm programming." Above 80 °C, the transition is complete, and the polymer enters its rubbery state. This region is very common for programming shape memory samples, known as "hot programming".

3.3. Shape memory effect

Table 1 shows the quantified parameters for a single cycle of shape fixity and shape recovery. All samples were programmed in a hot condition. The shape recovery decreased significantly with increasing foaming agent content. This is likely due to the increased density and size of air bubbles, which restrict the movement of polymer chains and hinder shape recovery. Additionally, the higher hole density leads to more defects and stress concentration sites, further affecting shape recovery. Our findings suggest that shape recovery is heavily influenced by the foam's morphology and porosity. The table also shows that all samples exhibited desirable shape fixity above 96 %. This finding suggests that the programming protocol has a significant impact on shape fixity, and it is likely that the weight percentage of foaming agent, morphology, and printability are all influenced by the protocol used. Table 1 also presents the quantitative results of shape recovery and shape fixity ratio for samples with 1 % wt AZO under different programming conditions. The shape fixity ratio decreases as the programming condition changes from hot to warm and cold. In contrast, the shape recovery ratio increases in the cold programming condition. The warm condition exhibits a balance between shape recovery and shape fixity. Hot programming shows better shape fixity because the material is loaded in a rubbery state, allowing for homogeneous spatial deformation of polymer chains, resulting in the maintenance of the elongated shape due to the transition from rubber to glass in cooling step, which limits molecular mobility and allows for higher energy storage. Cold programming involves three types of strain: elastic, viscoelastic, and viscoplastic. When the load is removed, the elastic strain is recovered immediately, and some viscoplastic strain can be recovered over time. However, this means that the rate of shape fixity in cold recovery is limited. As a result, a lower programming temperature leads to a weaker shape fixity ratio and faster shape recovery. In

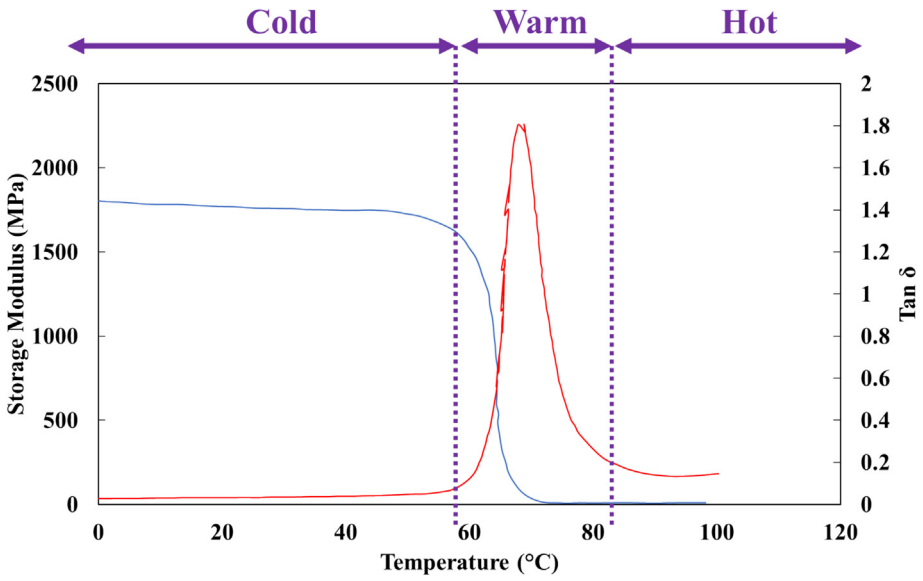

Fig. 3. DMTA results.

Table 1
Shape memory effect results.

AZO concentration	AZO%	Shape fixity	Shape recovery
	1	96.9	73.8
	3	96.4	48.3
	5	96.1	30.5
Programming temperature	Hot	96.9	73.8
	Warm	87.3	85.2
	Cold	75.1	90.3

addition, due to the closed-cell morphology of shape memory foams, homogeneous heat distribution in the inner layers is not possible and recovery is done at a lower rate. This issue is more challenging for hot programming than cold programming. Because in cold programming, the temporary shape is less stable and the driving force required for recovery is less. In addition, the dominant mechanism in cold shape memory is plastic deformation, and due to the homogeneous porous morphology, the possibility of deformation at ambient temperature is also available for brittle PLA. Therefore, in addition to the advantages of direct programming (no need for heating and cooling during the loading and unloading stages), cold programming facilitates the ability to achieve higher recovery for shape memory foams.

4. Concluding remarks

This study successfully demonstrated a novel approach to 4D printing of PLA shape memory foams, focusing on the effects of foaming agent content and programming temperature on their shape memory behaviors. The innovative method involved melt mixing PLA with azodicarbonamide below its decomposition temperature, followed by direct pellet printing at a higher temperature, enabling in-situ foaming. The main achievements and remarks are as follows:

- Morphological analysis confirms a uniform distribution of micropores.
- DMTA reveals a critical glass transition temperature around 65 °C.
- Higher AZO content enhances shape fixity (~96 %) but reduces shape recovery.
- Programming conditions significantly influences performance, with hot programming yielding better shape fixity and cold programming improving shape recovery.

CRediT authorship contribution statement

Pedram Honari: Writing – review & editing, Writing – original draft, Methodology, Investigation, Funding acquisition, Data curation. **Davood Rahmatabadi:** Writing – review & editing, Validation, Supervision, Project administration, Investigation, Formal analysis, Data curation. **Abbas Bayati:** Writing – review & editing, Writing – original draft, Validation. **Erfan Rassi:** Methodology, Data curation. **Ismaeil Ghasemi:** Supervision, Funding acquisition. **Majid Baniassadi:** Supervision, Funding acquisition. **Mahdi Bodaghi:** Methodology, Investigation, Writing – review & editing, Validation, Supervision. **Mostafa Baghani:** Supervision, Funding acquisition.

Declaration of competing interest

The authors declare that they have no known competing financial interests or personal relationships that could have appeared to influence the work reported in this paper.

References

[1] Aram E, Mehdipour-Ataei S. A review on the micro-and nanoporous polymeric foams: preparation and properties. Int J Polym Mater Polym Biomater 2016;65:358–75.
[2] Das P, Nayak PK, Muthusamy S, Kesavan RK. Foams for thermal insulation. In: Polym Foam Appl Polym Foam. ACS Publications; 2023. p. 145–65.
[3] Santo L. Shape memory polymer foams. Prog Aerosp Sci 2016;81:60–5.
[4] Zhang S, Gao Q, Zhang Y, Sheng X, Miao Z, Qin J, et al. 3D printing thermoplastic polyurethane hierarchical cellular foam with outstanding energy absorption capability. Addit Manuf 2023;76:. https://doi.org/10.1016/J.ADDMA.2023.103770103770.
[5] Bayati A, Rahmatabadi D, Ghasemi I, Khodaei M, Baniassadi M, Abrinia K, et al. 3D printing super stretchable propylene-based elastomer. Mater Lett 2024;361:. https://doi.org/10.1016/J.MATLET.2024.136075136075.
[6] Soleyman E, Rahmatabadi D, Soltanmohammadi K, Aberoumand M, Ghasemi I, Abrinia K, et al. Shape memory performance of PETG 4D printed parts under compression in cold, warm, and hot programming. Smart Mater Struct 2022;31:. https://doi.org/10.1088/1361-665X/AC77CB085002.